Desalination and Water Treatment
www.deswater.com

doi: 10.5004/dwt.2020.25885

195 (2020) 377–388
August

Synthesized chitosan–zeolite composite matrix for the adsorption of chromium(VI) ions

Ayokanni Adebayo Oshagbemi[a], Manase Auta[a], Abdulsalami Sanni Kovo[a], Muibat Diekola Yahya[a], Ambali Saka Abdulkareem[a], Mohammed Aris Ibrahim[a], Kehinde Shola Obayomi[b,*]

[a]*Department of Chemical Engineering, Federal University of Technology, Minna, Niger State, Nigeria, emails: ayocomes@yahoo.com (A.A. Oshagbemi), manaseauta@futminna.edu.ng (M. Auta), kovo@futminna.edu.ng (A.S. Kovo), muibat.yahya@futminna.edu.ng (M.D. Yahya), kasaka2003@futminna.edu.ng (A.S. Abdulkareem), ma.ibrahim@futminna.edu.ng (M.A. Ibrahim)*
[b]*Department of Chemical Engineering, Landmark University, Omu-Aran, Kwara State, Nigeria, Tel. +2348066967564; email: obayomi.kehinde@lmu.edu.ng (K.S. Obayomi)*

Received 22 October 2019; Accepted 23 March 2020

ABSTRACT

Chitosan–zeolite 3A composite (CS/Z) adsorbent was prepared to investigate the removal of Cr(VI) from aqueous solution. The chitosan (CS) was prepared from shrimp waste (shell) using chemical processes. The percentage yield and degree of deacetylation were 13.64% and 87.07%, respectively. The matrix formulation was obtained with a response surface methodology using a central composite design. The best matrix ratio of chitosan to zeolite was 1:7. This ratio was used for adsorption studies. Batch adsorption studies were carried out to investigate the optimum condition for the removal of Cr(VI) using CS/Z and the adsorbent was characterized using X-ray diffraction and scanning electron microscopy. The influences of solution pH, adsorption dosage, initial Cr(VI) concentration, and temperature on the removal processes were investigated. Adsorbent dosage of 0.25 g using 20 mg/L as the initial solution concentration showed maximum metal uptake, at optimum pH 2. The result obtained from equilibrium isotherm adsorption studies of Cr(VI) ion was analyzed in three adsorption models namely: Langmuir, Freundlich, and Temkin. The equilibrium studies carried out followed Langmuir isotherm with the highest correlation coefficient (R^2) value of 1. The kinetic parameters were evaluated utilizing the pseudo-first-order, pseudo-second-order, and Elovich-second-order. It was shown that the adsorption of Cr(VI) ions can be described by the Elovich kinetic model, with a correlation coefficient of 0.96. Thermodynamic parameters studies revealed that the adsorption process was spontaneous and endothermic in nature. In comparison between CS/Z, Z, and C, the percentage of removals were 97%, 68%, and 50%, respectively. Thus, it can be deduced that CS/Z composite adsorbent is effective and efficient for the removal of Cr(VI) ion.

Keywords: RSM; Ratio; Degree of deacetylation; Equilibrium; Kinetics; Thermodynamics studies

1. Introduction

Proliferation of industrialization especially in developing countries has led to continuous disposal of heavy metal into the environment. Heavy metals are a general collective term applying to the group of metals and metalloids with an atomic density ≥5 g cm^{-3} [1]. Widely recognized and used heavy metals such as chromium (Cr), cadmium (Cd), copper (Cu), mercury (Hg), nickel (Ni), lead (Pb), and zinc (Zn) are also toxic in nature. Unlike organic wastes, heavy metals are non-biodegradable and they can be accumulated in living

* Corresponding author.

1944-3994/1944-3986 © 2020 Desalination Publications. All rights reserved.

tissues, causing various diseases, and disorders, therefore they must be removed before discharge [2,3].

(Cr) compounds are used in many industries such as textile dyeing, tanneries, and metal electroplating. The heavy metal can exist mainly as Cr(VI) or Cr(III) in the natural environment. Cr(III) species is not toxic, less soluble, and more stable compare to Cr(VI) species which are highly soluble and mobile in aqueous solutions [4]. It has higher mobility than Cr(III) and therefore has a higher potential to contaminate the groundwater. The high risk of chromium(VI) is associated with its high reactivity and its potential carcinogenic properties [5]. Acute exposure to Cr(VI) causes nausea, diarrhea, liver and kidney damage, dermatitis, internal hemorrhage, and respiratory problems [6].

Various chemical and physical treatments have been developed (e.g., oxidation, reduction, precipitation, solvent extraction, membrane separation, ion exchange, and adsorption) for the removal of heavy metal ions from water bodies. Among these methods, the adsorption was considered to be the least expensive and very effective separation technique for the removal of metal ions present at low concentrations in industrial wastewater [7–9]. Adsorption process involves the use of suitable adsorbent for the targeted sorbate in the fluid. Conventional adsorbents often used include silica, activated alumina, coal, commercial activated carbon, clay, zeolite amongst others. In the past decades, research has brought to limelight the applicability of some agricultural waste, chitosan, and composite adsorbents for effective adsorption [10].

Chitosan is a linear-polymer and a biomaterial that is produced commercially by deacetylation of chitin, a structural element in the exoskeleton of crustaceans and cell walls of fungi. Chitosan is a linear-polymer of acetylamino-d-glucose. It is biodegradable, harmless to living things, and has many amino and hydroxyl groups that can chelate heavy metal ions [11]. Chitosan solubility in dilute acid solutions is obtained from chitin by removing the acetyl group (CH_3–CO). These materials can be used as adsorbents with little processing and available locally in large quantities [12]. Chitosan has excellent and distinctive biological and physiochemical properties making its reaction significantly more versatile than cellulose. It is non-toxic, renewable, biocompatible, biodegradable, non-immunogenic, and can form salts with inorganic and organic acids [11]. The presence of some amino (–NH_2) groups, hydroxyl (–OH) groups, and its chains flexibility makes it attractive for application in adsorption processes. However, it has both mechanical and chemical weaknesses which include dissolution in acids, gel formation in aqueous solution, the formation of the colloid solution with water, low surface area, low specific gravity, high cost, and susceptible to microbiological and biochemical degradation. These physical and chemical weaknesses can be alleviated to improve on its properties and applicability. Crosslinking, encapsulation, grafting can modify it chemically whereas its immobilization on another material reduces the quantity (cost) needed and enhances easy accessibility of its binding sites [13–15].

Zeolites are a microporous aluminosilicate mineral that occurs naturally or by synthesis and belongs to the class minerals known as "tectosilicate." They have unique properties and applications in ion exchange, catalyst, adsorption, and separation [16]. Zeolites are generally described as crystalline aluminosilicate based on their corner-sharing TO_4 (where T = Si and Al) tetrahedral which always form a three-dimensional framework with unique and uniform pore size [17].

Recently, several technologies using microorganisms, chitosan, and zeolite have been tested as ways of removing heavy metals from the environment. During the adsorption process of chitosan, the nitrogen from the amino group acts as an electron donor which is mainly responsible for the adsorption of metal ion [18].

[19] examined the removal of Cr(VI) by means of a bio-sorption onto coffee husk from aqueous solution. The effects of adsorbent dosage, pH, initial concentration, contact time, on the uptake of Cr(VI) were studied. The outcomes of the investigation established that after 60 min the adsorption of chromium by wheat bran attained. At a pH of 2, the maximum chromium uptake (87.8 %) was attained. The results obtained from the study, shows that Cr(VI) uptake onto wheat bran best fits the Langmuir isotherm model (R^2 = 0.997), and followed pseudo-second-order kinetic. The result obtained was an indication that the adsorbent used (wheat bran) can effectively replace other commercial adsorbents in the uptake Cr(VI).

The removal of hexavalent chromium from aqueous solutions onto synthetic nano-sized zero-valent iron (nZVI) was examined by [20]. It was observed from its findings that the removal efficiency increases with adsorbent dosage and contact time but resulted in a decrease with initial metal concentration and pH of the solution. The result confirmed the Langmuir model as the best fits as compared with other models studied. In Summary, to the best of our knowledge, no one has recorded excellent Cr(VI) uptake from the literature studied. Therefore, there is an essential need to achieve a better percentage of removal with minimal cost.

The advantages of Zeolite 3A is high-temperature support and good acid yield stability [21]. Numerous studies have shown that zeolites are good adsorbents for heavy metals uptake and their application in chitosan modifications has yielded positive results in wastewater treatment [17–18]. This study is aimed at determining the best chitosan–zeolite 3A composite matrix for of Cr(VI) uptake from wastewater. This involved preparation of chitosan from shrimps waste (shell), use of central composite design (CCD) for the formulation of the chitosan/zeolite 3A design matrix, application of the emerging composite for the adsorption of Cr(VI), and characterization of the composite adsorbent.

2. Materials and methods

2.1. Materials

All chemicals used for the experiments (acetic acid, HCl, potassium dichromate, and sodium hydroxide) were of analytical grade with purity between 80% and 99%. Shrimp shells were collected from Lagos lagoon, Nigeria. Chromium stock solution was prepared by measuring 2.835 g of 99% potassium dichromate ($K_2Cr_2O_7$) into 1.0 L volumetric flask, filling it up to the mark and then stirred until the solution was homogenous to give 1,000 mg/L Cr(VI) solution.

2.2. Synthesis of chitosan adsorbent

The shrimps shells collected were washed with water, scraped free of loose tissue, and were dried at room temperature for 10 d until it was well dried and crispy. The product was crushed with mortal to create shrimp shell powder. The particle sizes were determined by passing through mesh size (300 μm). Chitosan was synthesis from shrimp shells through three operation steps namely: demineralization, deproteinization, and deacetylation.

The 300 μm shrimp shells powder was soaked in a beaker containing 1 M HCl (1:10 w/v) at ambient temperature for 6 h after which it was washed in the acid until no bubbles were seen and no color change was observed. The sample was then washed thoroughly with distilled water until a neutral pH was obtained and then the demineralized shell was dried at 85°C for 18 h. The process of demineralization was followed by deproteinization.

The demineralized shrimp shell powder was transferred into a beaker containing 1 M NaOH solution (1:10 w/v) at ambient temperature and left for 16 h. The shells were then washed thoroughly with distilled water until a neutral pH of 6.8–7 was obtained. The deproteinized sample known as chitin was dried to constant weight, ground, and sieved into 300 μm for onward deacetylation.

The chitin sample was treated with 50% NaOH (1:10 w/v) for 3 h at 105°C using a heating mantle for deacetylation reaction. The deacetylated was then washed thoroughly with distilled water several times to remove residual NaOH until neutrality was attained. The resulting chitosan was then dried in the oven at 85°C for 15 has reported by Rahmani et al. [21].

The degree of deacetylation (DDA) of the various chitosan samples obtained was determined using Eq. (1):

$$\text{Percentage DDA} = 118.883 - \left[40.1647\left(\frac{A1655}{A3450}\right)\right] \quad (1)$$

where $A1655$ and $A3450$ are absorbance bands at 1,655 and 3,450 from the Fourier transform infrared (FTIR) spectra and are given by [22]:

$$A3450 = -\log\left(\frac{T3450}{100}\right) \quad (2)$$

$$A1655 = -\log\left(\frac{T1655}{100}\right) \quad (3)$$

2.3. Chitosan/zeolite composite matrix formation and its adsorption potential

CCD of response surface methodology (RSM) was used to formulate the chitosan/zeolite composite matrix. Range of the amount of the two factors chitosan (0.3–0.9 g) and zeolite (5–12 g) were obtained from preliminary investigations. The application of CCD with two factors and two levels gave a total of 13 experiments determined by the expression $2^n + 2n + 5$, where n is the number of factors. Percentage removal of chromium (VI) from aqueous solution was set as the response or independent variable while the dependent variables were the two factors chitosan and zeolite. To minimize the effect of unexpected variability on the observed responses, experimental runs were randomized. The CCD chitosan/zeolite composite matrix formation experimental design is presented in Table 1.

The composite matrix formulation was carried out by dissolving chitosan in 30 mL of 5% (v/v) HCl and stirred for 2 h at 200 rpm. Thereafter, the powdered zeolite was added to the dissolved chitosan solution stirred at 200 rpm until homogeneity was observed. The amount of chitosan and zeolite used was based on the CCD experiment design. The mixture was in drop-wise put into 1 M NaOH solution to form the composite beads which were later recovered and washed with distilled water to remove the adhering NaOH concentration. The beads were dried in an oven set at 85°C for 18 h and then packaged for use.

2.4. Batch adsorption studies

The effect of initial concentration and contact time on adsorption of Cr(VI) with CS/Z was studied by preparing 50 mL of the solute solution of 10, 20, 30, and 50 mg/L into five different 250 mL Erlenmeyer flasks. The Cr(VI) solution was adjusted to pH 2 and 0.2 g of CS/Z beads measured into each flask and placed into an isothermal water bath shaker set at 30°C and 150 rpm. The residual Cr(VI) concentration in the solution was determined at intervals by taking aliquot to a UV-Vis spectrophotometer of the wavelength of 540 nm. This was continued until the dynamic adsorption equilibrium was attained before terminating the experiment. The Cr(VI) uptake at equilibrium q_e (mg/g) was calculated as follows:

$$q_e = \frac{\left(C_0 - C_e\right)}{W} V \quad (4)$$

where C_0 (mg/L) is Cr(VI) initial concentration, C_e (mg/L) is the concentration at equilibrium, V (L) is the volume

Table 1
CCD for two independent variables used

Run/order	Chitosan (g)	Zeolite (g)	Ratio
1	0.55	8.00	1:15
2	0.55	8.00	1:15
3	0.20	8.00	1:40
4	0.80	11.0	1:14
5	0.30	5.00	1:17
6	0.55	8.00	1:15
7	0.55	8.00	1:15
8	0.55	8.00	1:15
9	0.55	12.24	1:22
10	0.55	3.76	1:7
11	0.90	8.00	1:9
12	0.80	5.00	1:6
13	0.30	11.0	1:37

of Cr(VI) solution, and W (g) is the weight of CS/Z beads. The procedure stated above was repeated by varying the isothermal experimental temperature to 40°C and 50°C in order to study the effect of temperature on the adsorption process.

The effect of solution pH on adsorption was studied by varying the pH values ranging from 2 to 12 in different Erlenmeyer flasks was 0.1 M HCl and NaOH. In each flasks, 50 mL of 20 mg/L Cr(VI) was measured into it and 0.25 g of CS/Z was added. The flasks were placed in water bath shaker set at 30°C and 150 rpm until the equilibrium time was attained. The residual solution concentration was determined using UV-Vis spectrophotometer.

Similarly, the effect of adsorbent dosage on Cr(VI) removal was studied by measuring 0.1, 0.25, 0.5, 0.75, 1.0, 1.25, and 1.5 g of the CS/Z beads separately into seven different flasks containing 50 mL of 20 mg/L with adjusted pH 2. The flasks were afterwards placed in a water bath shaker set at 30°C and 150 rpm until the equilibrium adsorption time of CS/Z was attained. The residual concentration of the various flasks was determined using the UV-spectrophotometer at 540 nm.

2.5. Characterization of chitosan, zeolite, and CS/Z

The morphology, functional groups, and the crystallinity of the synthesized chitosan, zeolite 3A, and their composite (CS/Z) were determined using scanning electron microscopy (SEM), FTIR, and X-ray diffraction (XRD) analyses, respectively.

2.5.1. SEM analysis

SEM (Philip XL40, Netherlands) was used to determine the morphology of the samples under vacuum conditions at a pressure of 5 bar. The samples were mounted over sample holder (stubs) aided by double-sided tape. Bio-Rad coating systems were used to further coat the sample with gold and this was carried out at 10–1 m bar with 30 mA of current flow or 75°. The samples were then placed into SEM instrument for scanning. Tungsten filament was utilized as an electron source and SEM micrograph was recorded with 10 Kv revolution to obtain 1,000×, and 7,000× magnification.

2.5.2. XRD analysis

The average bulk compositions and crystallinity of the chitosan and zeolites were determined using X-ray powder diffractometer with a Ni – filtered Cu Kα X-ray radiation source. One gram of each sample were air dried, homogenized, and placed on the sample holder of the machine for scanning. The samples were analyzed using the reflection–transmission spinner stage with the theta–theta settings. Two-theta (2θ) starting position was 0.00483° and ends at 75.96483° with a two-theta (2θ) step of 0.026° at 3.57 s per step. Tube current was 40 mA and the tension was 45 VA. Fixed divergent slit size of 10 was used and the goniometer radius was 240 mm.

2.5.3. FTIR analysis

The FTIR analyses of the samples were carried out from 4,000 to 400 cm^{-1} wavelength. The beads were mixed with potassium bromide (KBr) at a ratio of 1:19 crushed in a mortar and transformed into a disc with the aid of a pressure compressor. The disc produced was used for the FTIR analysis. The spectra generated were normalized and major vibrations bands were identified that were associated with the main groups.

3. Results and discussion

3.1. Chitosan yield

The percentage yield of chitosan from chitin after deacetylation was determined to be 13.64%. The DDA was approximately 87% which is considered agreeable compared to previously reported work where DDA of 87%–97% was achieved at different deacetylation conditions [22]. The properties of the synthesized chitosan are presented in Table 2. Recent developments in polysaccharide-based materials show that molecular weight and DDA are important characteristics of chitosan that influences its adsorption properties. The molecular weight and DD obtained in this study were 2.044×10^5 g/mol and 87.07%, respectively, which are comparable to the result (82.81% DD) obtained by No and Meyers [23]. The relatively high value of DD of chitosan obtained in this research shows that it can serve as a good adsorbent for adsorption [24]. The chitosan prepared was found to be soluble in 1% of acetic acid and hydrochloric acid concentration and insoluble in water. The buoyancy test also revealed that it floated on water successfully. The prepared chitosan was found to be soluble in 1% of acetic acid and hydrochloric acid, respectively, and insoluble in water. It is justified that the main physical differences between chitin and chitosan are the ability of chitosan to be soluble in organic acid such as acetic acid. The molecular weight and DD for the synthesized chitosan were 2.044×10^5 g/mol and 87.07%, respectively, which are similar to reported values of 2.044×10^5 g/mol and 82.81% [23].

3.2. Determination of best matrix formulation on adsorption capacity using design expert software

The experimental design CCD matrixes and the percentage removal of Cr(VI) are presented in Table 3. A total of 13 adsorption experimental runs were generated employing detailed conditions designed by RSM.

Table 2
Properties of the synthesized chitosan

Properties	Values
Color	Creamy white
Buoyancy in water	Buoyant
Solubility in water	Insoluble
Solubility in acetic acid	Soluble
Viscosity (cPs)	7
Molecular weight (g/mol)	2.044×10^5
DD (%)	87.07
pH	7.3
Surface	Smooth

Table 3
Experimental design CCD matrixes and the percentage removal of Cr(VI)

Run/order	Chitosan (g)	Zeolite (g)	Ratio	Actual removal (%)	Predicted removal (%)
1	0.55	8.00	1:15	71	71.00
2	0.55	8.00	1:15	71	71.00
3	0.20	8.00	1:40	59	58.99
4	0.80	11.0	1:14	69	68.80
5	0.30	5.00	1:17	65	66.45
6	0.55	8.00	1:15	71	71.00
7	0.55	8.00	1:15	71	71.00
8	0.55	8.00	1:15	71	71.00
9	0.55	12.24	1:22	62	63.15
10	0.55	3.76	1:7	79	76.60
11	0.90	8.00	1:9	77	75.76
12	0.80	5.00	1:6	78	80.31
13	0.30	11.0	1:37	60	58.94

The design was meant to enhance the best matrix formulation composite for the adsorption of Cr(VI) which was determined from the optimum synergy of the two materials via percentage removal values recorded. The effect of the synergy of the chitosan and zeolite on Cr(VI) was further depicted by the 3D response surface and contour plots are presented in Fig. 1. The slice shown includes five center points as indicated by the dot in the middle of the contour plot. By replicating center points, a very good power of prediction in the middle of the experimental region could be obtained. The best formulation that yielded the highest percentage of removal was at chitosan to zeolite ratio of 1:7. This shows that the zeolite served as the support for the chitosan bio-polymer that had high adsorption potentials.

3.3. Adsorbent characterization

3.3.1. X-ray diffractometry analysis of chitosan, zeolite, and CS/Z

The XRD analysis of Fig. 2 indicated that chitosan has crystalline and amorphous region, which confirmed the semi-crystallinity of chitosan. The XRD pattern exhibited strong diffraction peaks in the scattering range (2θ) at 18.3° and 24°, also a weak peak at 10°. This is comparable with the pattern of commercial chitosan with peaks at 20.07° and 81.71° (2θ) indicating it's amorphous and crystallinity nature, respectively [15]. Fig. 3 showed the diffractogram of chitosan–zeolite 3A composite. Compared with the diffractogram of only chitosan, the chitosan–zeolite composite indicate higher crystallinity. The introduction of zeolite 3A particles into matrices increased the crystallinity of the chitosan at 100, 120, 210, and 270 and also the thermal stability, although it decreases the flexibility. The X-ray diffractogram of CS/Z sample showed some characteristic peaks of both components (zeolite and chitosan) and the differences may be justified by the incorporation of zeolite crystals in the chitosan matrices [25,26].

3.3.2. SEM analysis

Figs. 4a–c present the morphology of the surface of the synthesized chitosan, CS/Z composite adsorbent before

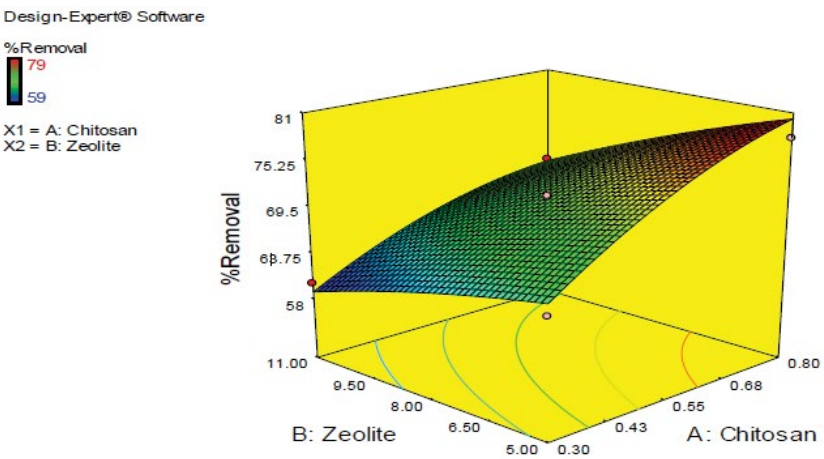

Fig. 1. Three-dimensional response surface plots.

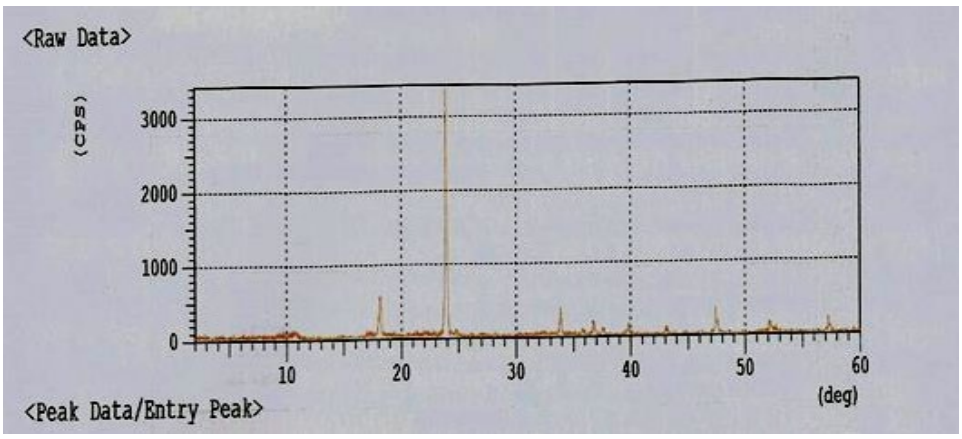

Fig. 2. XRD diffractogram of prepared chitosan.

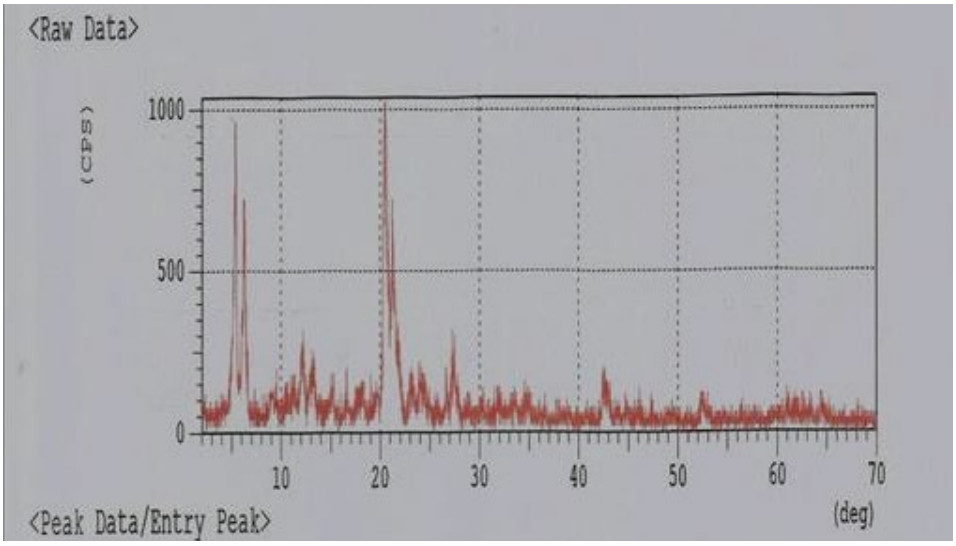

Fig. 3. XRD diffractogram of prepare chitosan–zeolite composite (best matrix).

adsorption, and CS/Z composite adsorbent after adsorption, respectively. Micrograph of synthesized chitosan has rough close-fitting surface morphology with minimum residues and sometimes as observed in this study a non-homogenous and non-smooth surface with straps and shrinkage [12]. Fig. 4b presents a great amount of well-formed cubic crystals with a very dull surface of the composite adsorbent which after adsorption shown in Fig. 4c reflected a shining (glittering) surface on the adsorbent and appeared closely packed, which indicates that Cr(VI) has been anchored (adsorbed) on the surface [27].

3.3.3. FTIR analysis

Fig. 5 presents the FTIR of synthesized chitosan. The expected functional groups in chitosan, a derivative of chitin after deacetylation were the free amino, the primary and secondary hydroxyl, and the ketones groups which have the bandwidth peak values. The wide band of $-NH_2$ at 3,423.76 cm^{-1} corresponds to N–H stretching vibrations of free amino groups. Similarly, the band observed at 2,921.29 cm^{-1} corresponds to CH stretching vibrations. The band at 1,072.46 cm^{-1} is as a result of stretching primary hydroxyl groups of tertiary O–H stretching. The band at 1,632.80 cm^{-1} corresponded C=O stretch of the carbonyl group, a structural feature of chitosan and the occurrence of deacetylation which are similar to the result obtained by [15]. This characteristic feature of carbonyl group overlap is not alone sufficient to determine the extent of deacetylation because there are ranges in frequency of carbonyl compound due to differences in classes which may be primary, secondary, or tertiary group [28]. The broad amino and hydroxyl band groups present enhanced the adsorption potential of the composite for the targeted Cr(VI) heavy metal [29].

3.4. Adsorption studies

3.4.1. Effect of pH on adsorption of chromium (VI) ion adsorption

The variation of adsorption of Cr(VI) on CS/Z observed with various pH indicated that potency of hydrogen had

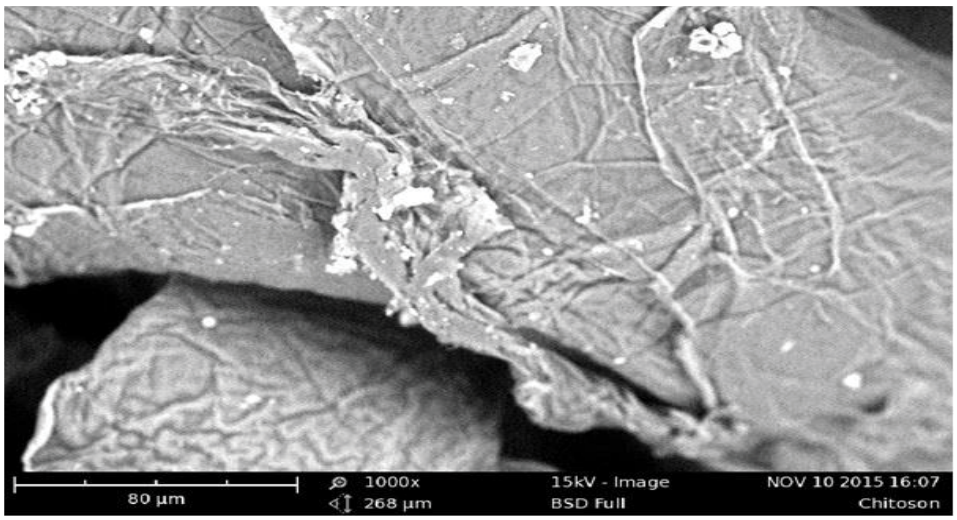

(a)

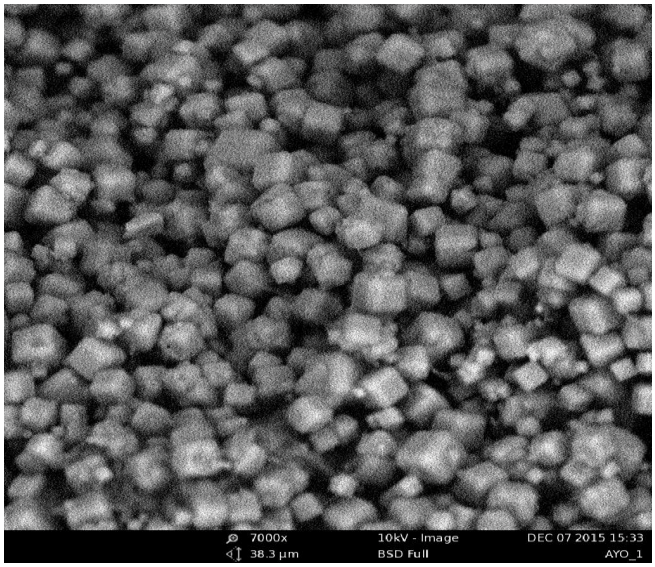

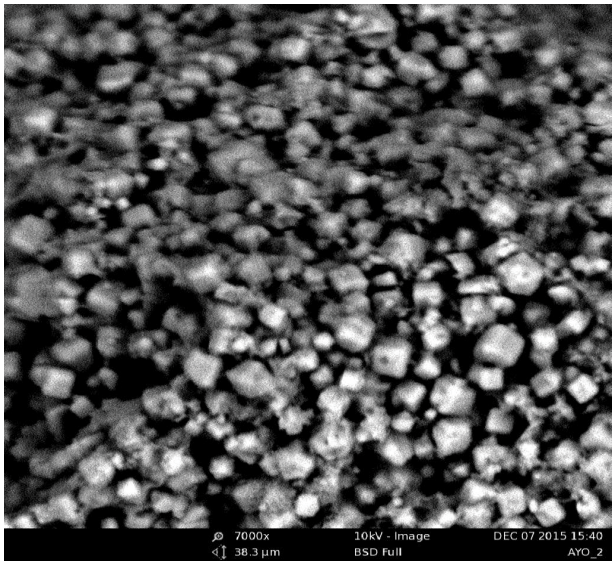

(b) (c)

Fig. 4. SEM images of (a) synthesized chitosan, (b) chitosan zeolite composite before adsorption, and (c) after adsorption

effect on the process. Stability of chromium is strongly dependent on the pH of the system as it can exist in different oxidation state with pH variation [12]. The protonation activities of CS/Z composite at low pH increased H^+ on its surface significantly and this promoted electrostatic attraction between the chromate ions and the positively charged adsorbent surface. Fig. 6 reveals maximum adsorption of Cr(VI) at pH 2 which may have been H_2CrO_4 [27,30], reported that in terms of preference of adsorption, H_2CrO_4 predominates $Cr_2O_7^-$, $Cr_3O_2^-$, $Cr_4O_2^-$, and $HCrO_4^-$ which are adsorbed at lesser acidic medium (pH 1–5) even though they coexist as presented:

$$H_2CrO_4 \leftrightarrow H^+ + H_2CrO_4^- \quad (5)$$

$$H_2CrO_4^{2-} \leftrightarrow H^+ + CrO_4^{2-} \quad (6)$$

$$2HCrO_4^- \leftrightarrow CrO_7^{2-} + H_2O \quad (7)$$

At pH > 6, the percentage removal drastically reduced (Fig. 6) which was attributed to repulsive activities and competition between the CrO_4^{2-} and OH^- (anions) for adsorption on the CS/Z surface [16]. The subjection of CS/Z composite at low pH (acidic medium) protonated amine ($-NH_2$) group on the surface to form $-NH_3^+$ facilitated electrostatic attraction between the negatively charged Cr(VI) and the positively charged polymer surface [24].

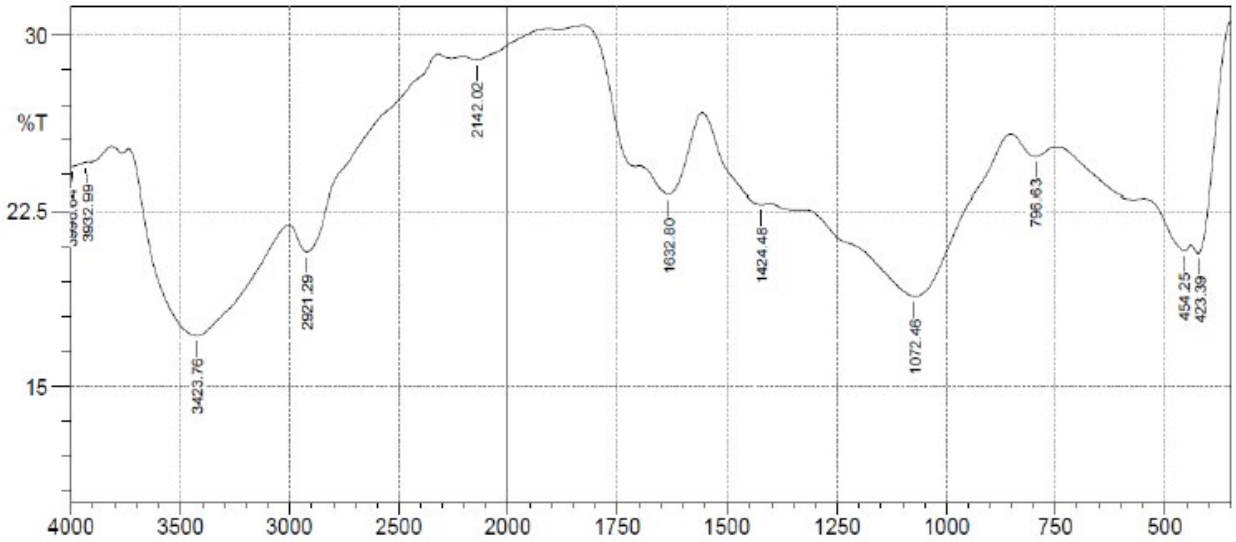

Fig. 5. Fourier transform infrared spectral of synthesized chitosan.

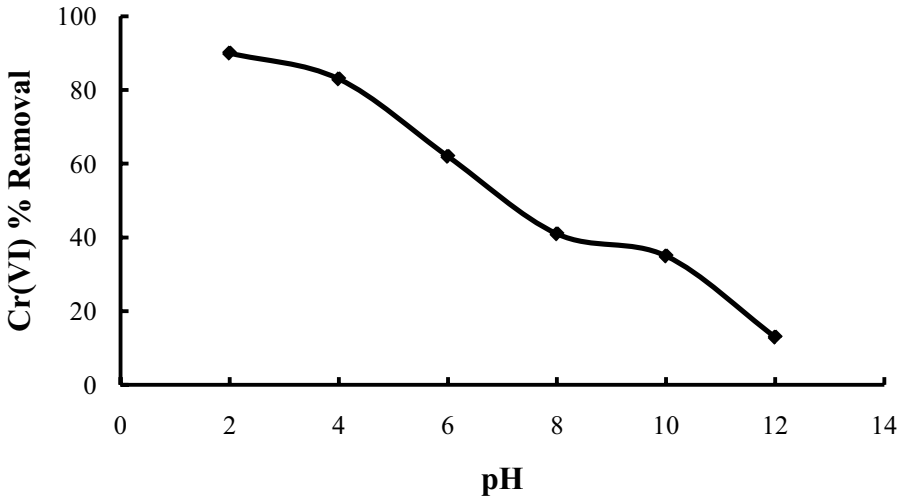

Fig. 6. Effect of pH on the adsorption of Cr(VI) onto CS/Z (experimental conditions: initial Cr(VI) concentration: 20 mg/L, adsorbent dose: 0.25 g/50 mL, agitation speed: 150 rpm, temperature: 301 K, contact time: 90 min).

$$-NH_2 \xleftrightarrow{H^+} -NH_3^+ \quad (8)$$

3.4.2. Effect of adsorbent dosage

The low Cr(VI) percentage uptake observed at 0.2 g CS/Z dosage was attributed to occurrence of competitive adsorption on the limited active site of the adsorbent. Significantly, the % Cr(VI) removal increased to 85% from 75% (Fig. 7). The observation was attributed to increase in availability of more active sites for adsorption and also increase in solution pH. More adsorbent connotes increase in the number of amine groups available for protonation activities which subsequently resulted to the rise in pH [24]. The Fig. 7 revealed that further increase in CS/Z polymer saturation increased dosage (>2.5 g) negated Cr(VI) adsorption on the surface. The increased dosage may have reduced the CS/Z polymer saturation with the limited concentration of the adsorbate.

3.4.3. Effect of initial concentration on Cr(Vl) ion adsorption

The variation of initial Cr(VI) concentration from 10 to 50 mg/L when other experimental conditions were kept constant significantly influenced the system mass transfer (figure not shown). Higher percentage removal (80%–92%) was observed for an initial Cr(VI) concentration range of 10–30 mg/L. This was due to preponderances of yearning vacant sites on the CS/Z surface in a solution of limited solute. However, the % removal was observed to be lower at higher initial concentration (>30 mg/L) studied. Intensified mass transfer driving force was enormous at higher concentration for the limited active vacant sites available

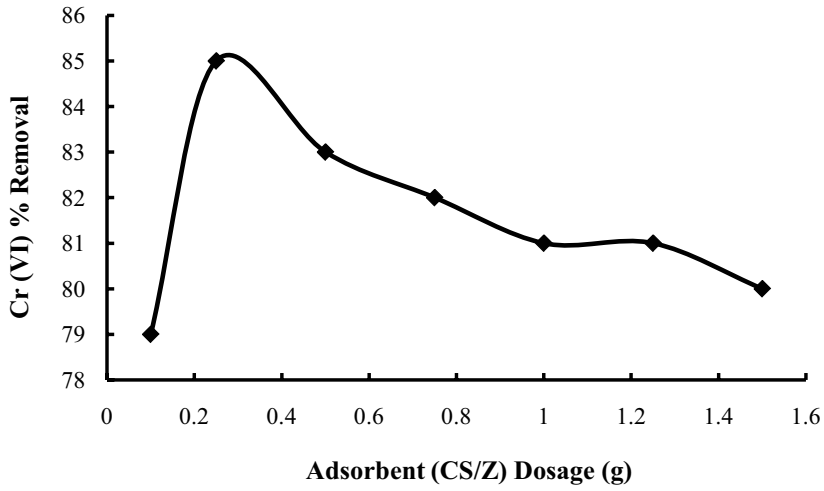

Fig. 7. Effect of adsorbent dosage on the adsorption of Cr(VI) onto CS/Z (experimental conditions: initial Cr(VI) concentration: 20 mg/L, agitation speed: 150 rpm, temperature: 301 K, contact time: 90 min).

leading to faster adsorbent concentration due to enhanced probability of collision between the sorbate molecules and the CS/Z surface [29].

3.4.4. Effect of temperature on Cr(VI) ion adsorption

Temperature plays a significant role in adsorption processes which suggest the process behavior on its variation. Profiles for Cr(VI) adsorption on CS/Z at different temperatures (30°C, 40°C, and 50°C) and concentrations varied from 10 to 50 mg/L when other operating condition were kept constant are illustrated in Fig. 8. It was observed that adsorption of Cr(VI) on CS/Z was enhanced as the temperature was increased. High temperature promoted excitement of Cr(VI) molecules which led to faster rate of their diffusion from the aqueous solution to the adsorbent [24].

3.5. Adsorption isotherms

The study of the equilibrium relationship of the distribution of the amount of Cr(VI) adsorbed and the amount being described was determined through application of some popular isotherm models. Application of such model equations to experimental data generated provides accurate mathematical description of the equilibrium adsorption capacity of any adsorbent [24]. This is indispensable for prediction of adsorption capacity parameters and for evaluation of both qualitative and quantitative adsorption behavior of adsorbents.

Langmuir, Freundlich, and Temkin isotherms models were fitted into the experimental data generated for Cr(VI) adsorption on CS/Z (figures are not shown). The resulting isotherm model plot parameters and the correlation coefficient (R^2) between the experimental and the models data provide valuable information on solute–adsorbent surface interaction and gives further information on the favorable or unfavorable nature of the adsorption process under study. Langmuir isotherm best fitted the experimental data generated for Cr(VI) adsorption on CS/Z than Temkin and Freundlich models. This was adjudged by the correlation coefficient (R^2) values of the model which were higher (closer to unity) than that of other models studied. The conformity of the experimental data to Langmuir model connotes that adsorption of Cr(VI) on to the CS/Z was monolayer, all active sites present were identical and equivalent energetically, the CS/Z has a finite capacity for the Cr(VI), and the CS/Z is structurally homogeneous [31].

The values of the isotherms model parameters studied are presented in Table 4. The Langmuir R_L which is a vital dimensionless factor parameter had a value of 0.037 connoting favorable adsorption isotherm studies. The value of R_L indicates the type of isotherm to be either unfavorable ($R_L > 1$), linear ($R_L = 1$), and favorable ($0 < R_L < 1$) or irreversible ($R_L = 0$). It is a positive number whose magnitude determines the feasibility of an adsorption process [32].

3.6. Adsorption kinetic studies

Adsorption rate of a pollutant by an adsorbent is an invaluable factor besides its capacity in the evaluation of the process. Three kinetic models were used to investigate their fitness to the experimental data generated (profiles of their plots are not shown). The selection of pseudo-first-order (Lagergren model), pseudo-second-order [33], and

Table 4

CS/Z adsorption isotherm value

	Parameter	Value
Langmuir	b	2.8
	R_L	0.037
	R^2	1.0000
Freundlich	K_f	2.3734
	$1/n$	0.5024
	R^2	0.9675
Temkin	K_T	0.9994
	b_T	–3,732.97
	R^2	0.9876

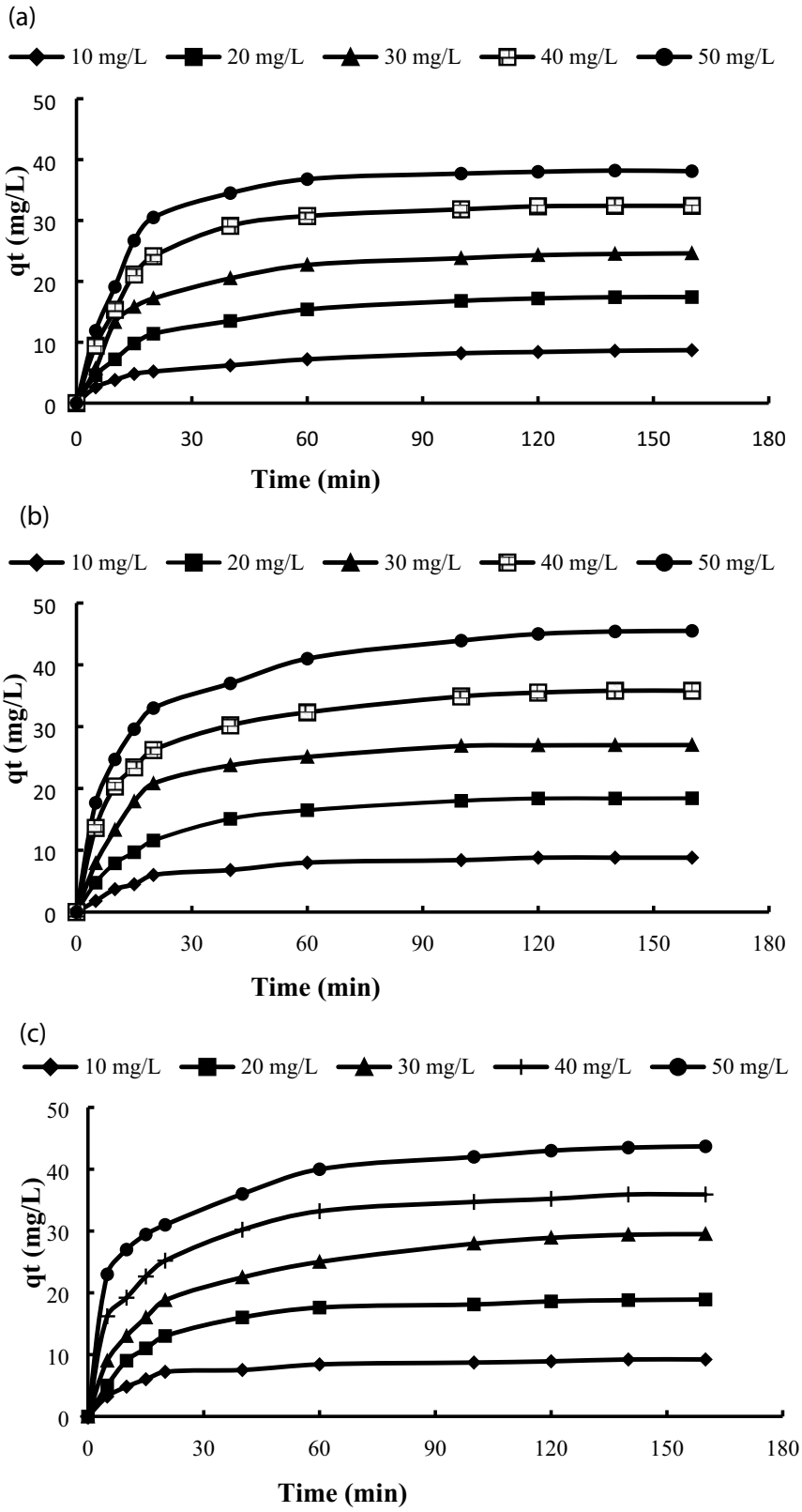

Fig. 8. Effect of temperature on Cr(VI) adsorption at (a) 30°C, (b) 40°C, and (c) 50°C.

Table 5
Evaluated constants obtained from the tested kinetic model for CS/Z

Model	R^2	Slope	Intercept	k	Other constants
Second-order	0.8909	0.3	0.062	0.000006	C_0 = 161.29
Pseudo-second-order	0.8909	–0.004	0.9429	222.265	q_e = 1.0606
Elovich	0.9562	–0.7295	65.674	b = –1.3708	A = 5.8246E-40
Pseud-first-order	0.6528	0.0076	–0.8286	1.9083	q_e = 0.1484

Elovich models considered the fact that adsorption can either be physical or chemical in nature. Evaluation of the three models parameters through fitting the experimental data revealed that the controlling mechanism of adsorption of Cr(VI) onto the CS/Z surface was best described by the Elovich model. This was adjudged by the high correlation coefficient (R^2) values as compared to the other models investigated. The best fitting of the experimental data to Elovich suggests that chemisorption was probably rate-controlling mass transfer mechanism of Cr(VI) onto CS/Z [34,35]. The kinetic models parameters are presented in Table 5. The experimental data best fitted into the Elovich kinetic model with highest R^2 value of 0.9949.

3.7. Thermodynamics of adsorption

Energy and entropy factors are considered invaluable in environmental engineering studies as they assist in determining processes that are spontaneous. Thermodynamic parameters such as Gibb's free energy $\Delta G°$, the enthalpy $\Delta H°$, and the entropy $\Delta S°$ were evaluated as they are the actual indicators for the practical applications of a process. LogK_d vs. $1/T$ was plotted to evaluate $\Delta H°$ and $\Delta S°$ from the slope and intercepts, respectively (Figure not shown). The Gibbs free energy ($\Delta G°$) of the adsorption process was –3.8553 kJ/mol which indicated that sorption of Cr(VI) on to CS/Z was feasible and spontaneous [36]. The positive values of $\Delta H°$ (2.0463 kJ/mol) and $\Delta S°$ (0.04468 kJ/mol) indicated that the adsorption activities were endothermic and were promoted with an increase in the degree of randomness of the adsorbed Cr(VI) molecules [37].

4. Conclusion

A semi-crystallized structure of chitosan was successfully synthesized from shrimps with over 87% DDA. Optimum chitosan–zeolite composite matrix (1:7) formulated was used for the removal of Cr(VI) ions from aqueous solution established the adsorbent capability in adsorbing at low sorbate concentration. Langmuir isotherm model best fitted the adsorption experimental data generated and the thermodynamic studies revealed that the adsorption process was spontaneous and endothermic. This study further affirmed that composite adsorbent should be preferred to mono-component sorbent materials.

References

[1] W.O. David, B. Colin, F.O. Thomas, Heavy metal adsorbents prepared from the modification of cellulose: a review, Bioresour. Technol., 99 (2008) 6709–672.
[2] F. Umar, A.K. Misbahul, A. Makshoof, J.A. Kozinski, Effect of modification of environmentally friendly biosorbent wheat (*Triticum aestivum*) on the biosorptive removal of cadmium(II) ions from aqueous solution, Chem. Eng. J., 171 (2011) 400–410.
[3] P. Xing, C. Wang, B. Ma, B.Y. Chen, Removal of Pb(II) from aqueous solution using a new zeolite-type absorbent: potassium ore leaching residue, J. Environ. Chem. Eng., 6 (2018) 7138–7143.
[4] W.S. Wan Ngah, M.A.K.M. Hanafiah, Removal of heavy metal ions from wastewater by chemically modified plant wastes as adsorbents: a review, Bioresour. Technol., 99 (2018) 3935–3948.
[5] P. Waranusantigul, P. Pokethitiyook, M. Kruatrachue, E.S. Upatham, Kinetics of basic dye (methylene blue) biosorption by giant duckweed (*Spirodela polyrrhiza*), Environ. Pollut., 125 (2003) 385–392.
[6] Y.A.B. Neolaka, G. Supriyanto, H. Darmokoesoemo, H.S. Kusuma, Adsorption performance of Cr(VI)-imprintedpoly(4-VP-co-MMA) supported on activated Indonesia (Ende-Flores) natural zeolite structure for Cr(VI) removal from aqueous solution, J. Environ. Chem. Eng., 175 (2018) 376–390.
[7] D. Mohan, C.U. Pittman, Activated carbons and low cost adsorbents for remediation of tri- and hexavalent chromium from water, J. Hazard. Mater., 137 (2006) 762–811.
[8] X. Liu, D. Lee, Thermodynamic parameters for adsorption equilibrium of heavy metals and dyes from wastewaters, Bioresour. Technol., 160 (2014) 24–31.
[9] K. Nakamoto, M. Ohshiro, T. Kobayashi, Mordenite zeolite—polyethersulfone composite fibers developed for decontamination of heavy metal ions, J. Environ. Chem. Eng., 5 (2017) 513–525.
[10] N.H. Mthombeni, S. Mbakop, S.C. Ray, T. Leswifi, A. Ochieng, M.S. Onyango, Highly efficient removal of chromium (VI) through adsorption and reduction: a column dynamic study using magnetized natural zeolite-polypyrrole composite, J. Environ. Chem. Eng., 323 (2018) 234–254.
[11] M. Auta, B.H. Hameed, Chitosan-clay composite as highly effective and low-cost adsorbent for batch and fixed-bed adsorption of methylene blue, Chem. Eng. J., 237 (2014) 352–361.
[12] M. Auta, B.H. Hameed, Coalesced chitosan activated carbon composite for batch and fixed-bed adsorption of cationic and anionic dyes, Colloids Surf., B, 105 (2013) 199–206.
[13] N.A. Oladoja, I.A. Ololade, S.E. Olaseni, V.T. Olatujoye, O.S. Jegede, O. Agunloye, Synthesis of nano calcium oxide from a gastropod shell and the performance evaluation for Cr(VI) removal from aqua system, Ind. Eng. Chem. Res., 51 (2012) 639–648.
[14] W.S. Wan Ngah, S. Fatinathan, Adsorption of Cu(II) ions in aqueous solution using chitosan beads, chitosan–GLA beads and chitosan–alginate beads, Chem. Eng. J., 143 (2008) 62–72.
[15] L. Zhou, Z. Liu, J. Liu, Q. Huang, Adsorption of Hg(II) from aqueous solution by ethylenediamine-modified magnetic crosslinking chitosan microspheres, Desalination, 258 (2010) 41–47.
[16] A.S.K. Kumar, S.J. Jiang, Chitosan-functionalized graphene oxide: a novel adsorbent an efficient adsorption of arsenic from aqueous solution, J. Environ. Chem. Eng., 4 (2016) 1698–1713.
[17] N. Jiang, R. Shang, S.G.J. Heijman, L.C. Rietveld, Highsilica zeolites for adsorption of organic micro-pollutants in water treatment: a review, Water Res., 180 (2018) 76–90.

[18] M. Hong, L. Yu, Y. Wang, J. Zhang, Z. Chen, L. Dong, Q. Zan, R. Li, Heavy metal adsorption with zeolites: the role of hierarchical pore architecture, Chem. Eng. J.,125 (2018) 456–476.
[19] R.N. Aleksandra, J.V. Saya, G.A. Dusan, Modification of chitosan by zeolite A and adsorption of bezactive orange 16 from aqueous solution, Compos. Part B, 53 (2013) 145–151.
[20] N. Ahalya, R.D. Kanamadi, T.V. Ramachandra, Removal of hexavalent chromium using coffee husk, Int. J. Environ. Pollut., 43 (2010) 106–116.
[21] A.R. Rahmani, M.T. Samadi, R. Noroozi, Hexavalent chromium removal from aqueous solutions by adsorption onto synthetic nano size zero valent iron (nZVI), World Acad. Sci. Eng. Technol., 50 (2011) 80–83.
[22] A. Gaffer, A.A. Al Kahlawy, D. Aman, Magnetic zeolite-natural polymer composite for adsorption of chromium(VI), Egypt. J. Pet., 6 (2017) 94–102.
[23] H.K. No, S.P. Meyers, Preparation and characterization of chitin and chitosan-a review, J. Aquat. Food Prod. Technol., 4 (1995) 27–52.
[24] E.S. Abdou, K.S. Nagy, M.Z. Elsabee, Extraction and characterization of chitin and chitosan from local sources, Bioresour. Technol., 99 (2008) 1359–1367.
[25] H. El-Knidri, R. Belaabed, A. Addaou, A. Laajeb, A. Lahsini, Extraction, chemical modification and characterization of chitin and chitosan, Int. J. Biol. Macromol., 120 (2018) 1181–1189.
[26] G. Crini, P. Badot, Application of chitosan, a natural amino-polysaccharide, for dye removal from aqueous solutions by adsorption processes using batch studies: a review of recent literature, Prog. Polym. Sci., 33 (2008) 399–447.
[27] A. Djelad, A. Morsli, M. Robitzer, A. Bengueddach, F. di Renzo, F. Quignard, Sorption of Cu(II) ions on chitosan-zeolite X composites: impact of gelling and drying conditions, Molecules, 21 (2016) 109.
[28] A. Morsli, A. Bengueddach, F. di Renzo, F. Quignard, Zeolite-chitosan composites: promising materials for catalysis and separation, Stud. Surf. Sci. Catal., 174 (2008) 1143–1146.
[29] E. Malkoc, Y. Nuhoglu, Fixed bed studies for the sorption of chromium(VI) onto tea factory waste, Chem. Eng. Sci., 61 (2006) 4363–4372.
[30] B. Palla-Rubio, N. Aráujo-Gomes, M. Ferńand ez-Gutíerrez, L. Rojo, J. Suay, M.M.I. Gurruchaga, Gõni, Synthesis and characterization of silica-chitosan hybrid materials as antibacterial coatings for titanium implants, Carbohydr. Polym., 203 (2018) 331–341.
[31] G.Z. Kyzas, D.N. Bikiaris, Recent modifications of chitosan for adsorption application: a critical and systematic review, Mar. Drugs, 13 (2015) 312–337.
[32] N. Zhao, N. Wei, J. Li, Z. Qiao, J. Cui, Surface properties of chemically modified activated carbons for adsorption rate of Cr(VI), Chem. Eng. J., 115 (2005) 133–138.
[33] K.S.P. Kumar, E.C.N. Peter, Adsorption of chromium(VI) from aqueous solutions by different admixtures – a batch equilibrium test study, J. Eng. Sci. Technol., 9 (2014) 410–422.
[34] M. Auta, B.H. Hameed, Preparation of waste tea activated carbon using potassium acetate as an activating agent for adsorption of Acid Blue 25 dye, Chem. Eng. J., 171 (2011) 502–509.
[35] Y.S. Ho, S. McKay, Pseudo-second order model for sorption processes, Proc. Biochem., 34 (1999) 451–465.
[36] K.S. Obayomi, M. Auta, A.S. Kovo, Isotherm, kinetic and thermodynamic studies for adsorption of lead(II) onto modified Aloji clay, Desal. Water Treat., 181 (2020) 376–384.
[37] K.S. Obayomi, M. Auta, Development of microporous activated Aloji clay for adsorption of lead(II) ions from aqueous solution, Heliyon, 5 (2019) e02799.